J Radioanal Nucl Chem (2017) 311:1155–1162
DOI 10.1007/s10967-016-5010-3

A comparative study on sorption and diffusion of Cs in crushed argillite and granite investigated in batch and through-diffusion experiment

Chuan-Pin Lee[1] · Shih-Chin Tsai[2] · Ming-Chee Wu[1] · Tsuey-Lin Tsai[3] · Yu-Lin Tu[1] · Ling-Jen Kang[1]

Received: 31 May 2016 / Published online: 30 September 2016

Abstract The batch and through-diffusion experiments in this study were conducted and compared in order to investigate the sorption and diffusion of cesium (Cs) for two potential host rocks in Taiwan: argillite from Taitung and granite from Kinmen Island, with the purpose of establishing a reliable safety-performance assessment methodology for the final disposal of low level radioactive waste. The results of Cs mapping by scanning electron microscope equipping by energy dispersive spectrometer (SEM–EDS) showed that the distribution of Cs on argillite and granite were enriched in illite and biotite, respectively. In addition, it showed that higher sorption capacities were found for argillite than granite; due to the clay mineral content (illite) in the argillite. Experiments for diffusion of Cs is agreement to the values estimated for the diffusive results (D_a) of Cs in argillite were revealed to be lower than those of granite.

Keywords Sorption · Diffusion · Cs · Argillite · Granite · Distribution coefficients

✉ Shih-Chin Tsai
sctasi@mx.tnhu.edu.tw

[1] Department of Earth Sciences, National Cheng Kung University, Tainan 70101, Taiwan

[2] Nuclear Science and Technology Development Center, National Tsing Hua University, Hsinchu 30013, Taiwan

[3] Chemistry Divisions, Institute of Nuclear Energy Research, Taoyuan 32546, Taiwan

Introduction

After the 2011 Fukushima Daiichi nuclear crisis, the Taiwan government (namely AEC, the Atomic Energy Council) and its designated operator Tai-Power Company (TPC) announced in November of that year permission to begin decommissioning the three nuclear plants (total 6 nuclear units) in Taiwan. The oldest operating nuclear units are the two 604 MW general electric boiling water reactors at Chinshan plant, which started commercial operation in 1978 and 1979. Moreover, there are three operating nuclear power plants on the island of Taiwan, and it was stipulated that the two advanced boiling water reactors (ABWR) under construction at Lungmen plant would only be allowed to start up after passing strict safety evaluations both by the government and international nuclear safety organizations.

For long-term performance assessment of the high level radioactive waste (HLW) or the low level radioactive waste (LLW) repository site, it is necessary to deal with issues related to the fact such as the waste is radiotoxic, has a long half-life (in the case of HLW and LLW), and whether it may transmit of radionuclides into the environment. A geological survey for natural barriers in Taiwan was proposed several years ago in order to determine the suitability of the proposed sites for final disposal of low-level radioactive wastes. Some geological investigations with research and development (R&D) on the radionuclide migration have been conducted [1–3]; and 2 candidate sites for LLW final disposal were announced by AEC 2 years ago including Kingman island and Taitung county, located at latitudes and longitudes of 24°N 118°E and 22°N 120°E, respectively as Fig. 1.

For low-level radioactive waste management, due to the long half-life and high activity dose, ^{137}Cs, is the essential

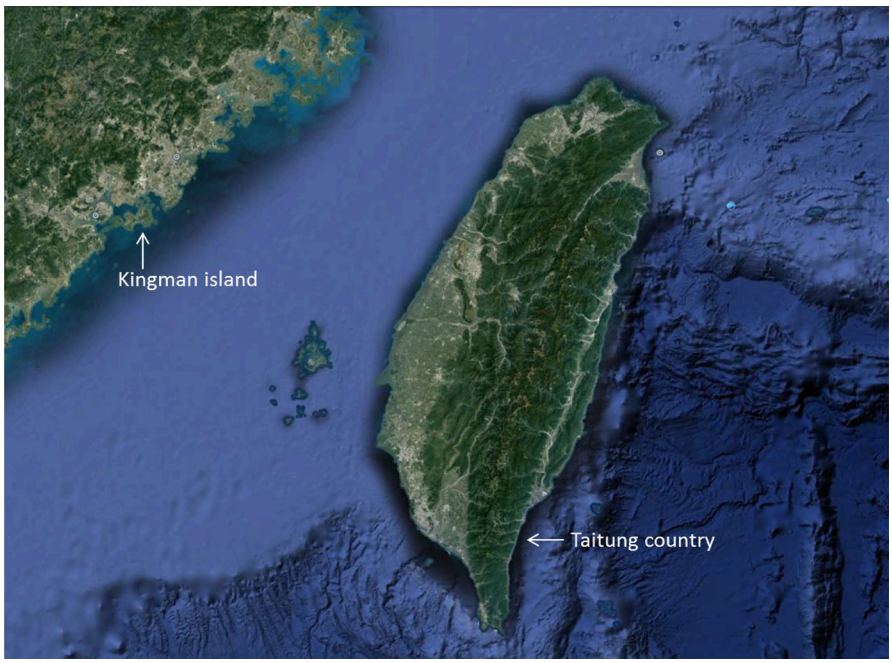

Fig. 1 Locations of Kingman island and Taitung country

elements studied by most countries. Namely, the buffer materials filled in around the solidified radioactive wastes will play a very important role in retarding the migration of radioactive nuclides as well as stabilizing the solidified radioactive wastes. According to the related studies, migration of radioactive nuclides in host rocks will be affected by the retardation effect caused by the adsorption mechanism of in situ rocks and minerals. The previous studies [4, 5] that have been conducted have primarily focused on the absorption mechanism of granite and basalt related to Cs and other radionuclides. According to the previous geological investigation, the sorption and diffusion behaviour of Cs on granite and mudrock has been studied and reported in literature [6, 7] and biotite and clay minerals might display as a major mineral component leading to the sorption of ^{137}Cs. Recently, a quantitative analysis of the major elements in geological materials, such as apatite and titanite, was provided and developed by an electron probe micro-analyzer (EPMA) or back-scattered electron (BSE) microscope analysis [8].

In this study, the sorption and diffusion behaviour of Cs in argillite (A) and granite (G), two local host rocks in Taiwan, were investigated using batch sorption and through-diffusion experiments. Moreover, an mapping analysis of Cs in argillite and granite by scanning electron microscope equipped with an energy dispersive spectrometer system (SEM–EDS) was provided and compared with polar microscopy. In order to obtain more accurate diffusion coefficients (D_a), the crushed rocks were compacted and also analysed simultaneously in through-diffusion experiments.

Experimental procedure

Rocks

Two potential host rock samples were collected and tested, i.e.: (1) approximately 3 kg argillite samples were collected from the Dazen Township of Taitung County at an outcrop along the Fongkang River, and (2) approximately 1 kg granite rock core samples were collected from the Wuchiu discrete islands of Kinmen by the Industrial Technology Research Institute (ITRI).

Pretreatment and N_2-BET specific surface area analysis

In this study, before use, all rock samples were crushed, sieved, and separated into three size groups: ~20–100 mesh (~0.149–0.833 mm), ~100–200 mesh (~0.074–0.149 mm), and <200 mesh (<0.074 mm). They were then washed three times using de-ionized water (DIW) and dried at 105 °C for 24 h. Then, the powder argillite and granite were also performed with N_2-BET (ASAP 2020, USA). It showed that the specific surface area of argillite (6.44–9.13 $m^2\ g^{-1}$) was higher than granite (0.07–1.96 $m^2\ g^{-1}$) in different particle sizes.

XRD and XRF analysis

A mineral analysis of argillite and granite was investigated by powder X-ray diffraction (XRD, D8 Advance, Bruker, Germany) and elemental analysis by X-ray fluorescence

(WDXRF, PANalytical, The Netherlands). The chemical components of argillite and granite are shown in Table 1. XRD spectra were compared with those in the International Center for Diffraction Data (JPCDS) database. This showed that major mineral composition of argillite and granite included quartz (A and G), plagioclase (A and G), feldspar (A and G), goethite (G), biotite (G), and illite (A) among other components. The predominant elements of argillite and granite present as oxides, as determined by XRF, were SiO_2, Al_2O_3, K_2O, Na_2O, CaO MnO, MgO, TiO_2, P_2O_5 and Fe_2O_3.

Table 1 Elemental composition of argillite and granite by XRF analysis

Composition	Argillite	Granite
SiO_2	61.62	60.43
Al_2O_3	18.38	14.47
Fe_2O_3	6.71	7.19
CaO	0.60	4.98
Na_2O	1.69	2.75
K_2O	3.04	3.29
MnO	0.06	0.14
MgO	2.54	2.89
TiO_2	0.80	1.07
P_2O_5	0.15	0.41
LOI	5.8	1.05

LOI loss in ignition

Polar-microscopy and SEM–EDS analysis

After pre-treatment by DIW, the argillite and granite samples were cutted, polished and glued onto a glass plate and then samples were then submerged into the stock solution, containing Cs with a concentration of about 0.04 M. After 7 days of immersion, the samples were taken out and rinsed quickly with DIW to remove Cs solution on the sample surface. After drying, the polar morphology of argillite and granite were observed, and the major sorption of Cs on both rocks was identified and compared in a scanning electron microscope (SEM, Model S-4800, Hitachi, Japan) equipped with an energy dispersive spectrometer (EDS, Horiba E-MAX, Japan) with an accelerating voltage of 20 kV and a current of 10 μA. The EDS was used to analyze the corresponding elemental composition of the argillite and granite.

Batch sorption experiments

The distribution coefficients (K_d) of the Cs ions for crushed argillite and granite were estimated using an ASTM batch method [9]. An aqueous solution with a volume of 30 mL containing 10 ppm Cs ion was contacted with 1 g of crushed rocks at 25 ± 1 °C for up to 7 days, which was found

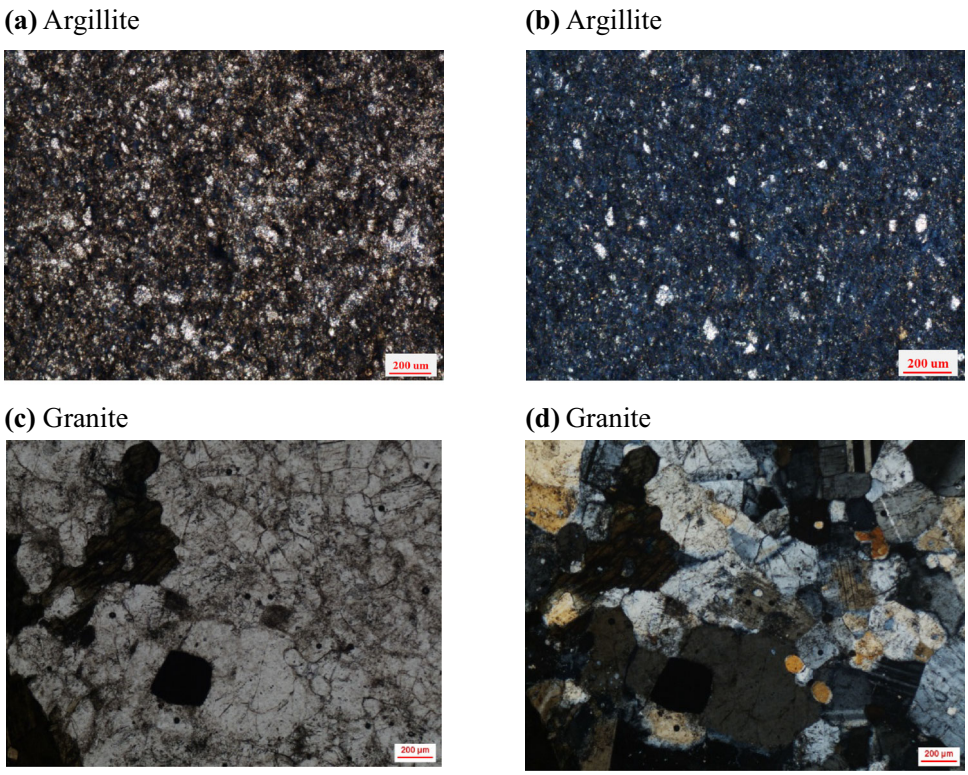

Fig. 2 Images of polar microscopy in argillite and granite. **a**, **c** Plane polarized light; **b**, **d** crossed polarized light; in polar microscopy

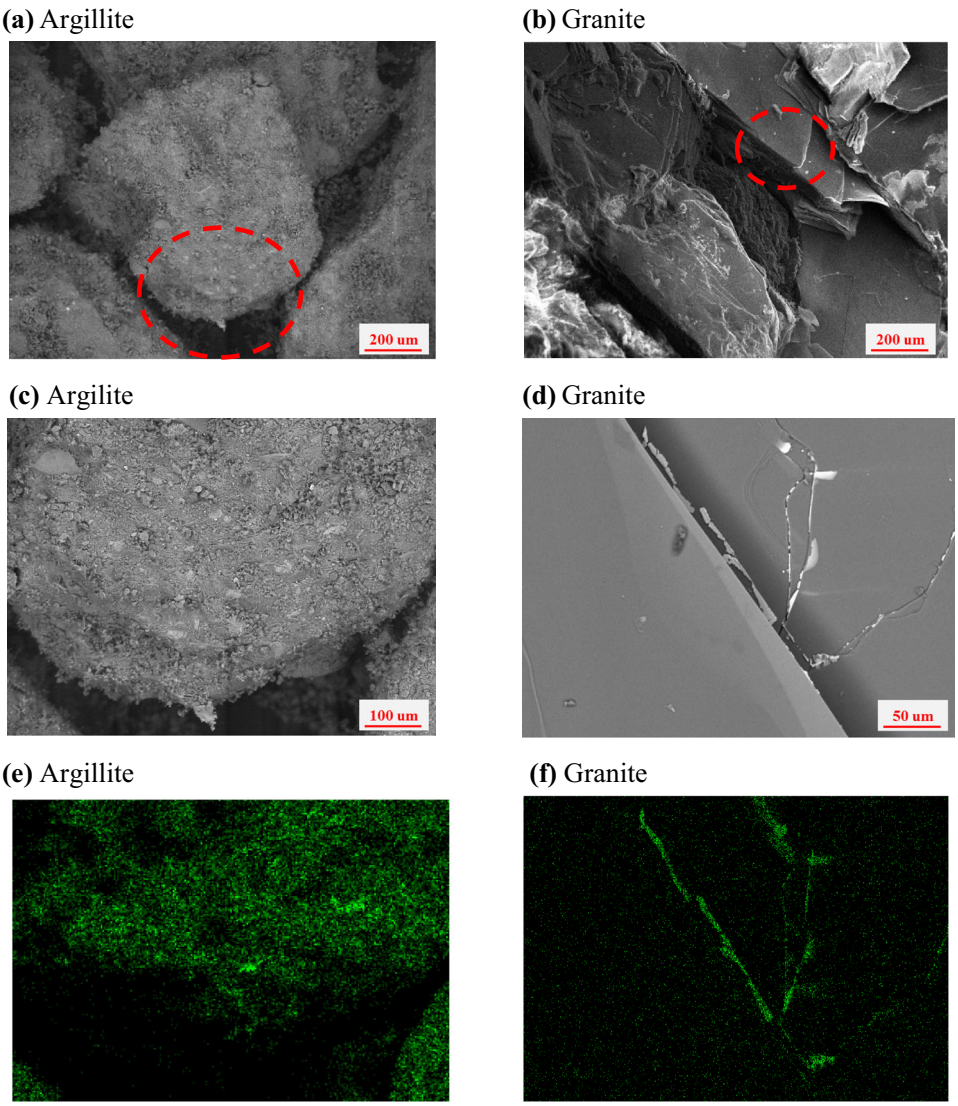

Fig. 3 SEM-EDS images and Cs mapping analysis (*green area*) of the surface on argillite and granite. **a**, **c**, **e** Argillite; **b**, **d**, **f** granite. (Color figure online)

Table 2 The specific surface area (SSA) and distribution coefficients (K_d) of Cs in argillite and granite in different particle sizes

Particle size (mm)	Argillite		Granite	
	SSA (m^2/g)	K_d (mL/g)	SSA (m^2/g)	K_d (mL/g)
0.149–0.833	6.44	166	0.07	8.77
0.074–0.149	7.13	79	0.21	3.13
<0.074	9.13	189	1.96	8.91

to be sufficient for attaining equilibrium. In order to check the interference of Cs sorption on the crushed rocks in different particle size, 3 part of particle sizes were also examined and analysed after 7 days. The concentrations of Cs ions in the solution were measured with a flame atomic absorption spectrometer (Thermo SOLAAR iCE 3300AA, Germany).

The distribution coefficient (K_d, cm^3/g) are defined as:

$$K_d = ((C_0 - C_f)/C_f) \times V/m, \quad (1)$$

where C_0, C_t and C_f (ppm) are the initial concentration of Cs, at time t, and at equilibrium, respectively; m (g) is the weight of the rock samples, and V (cm^3) is the volume of solution.

Through-diffusion experiments

Through-diffusion experiments were designed to determine diffusion coefficients for evaluating the migration of Cs in

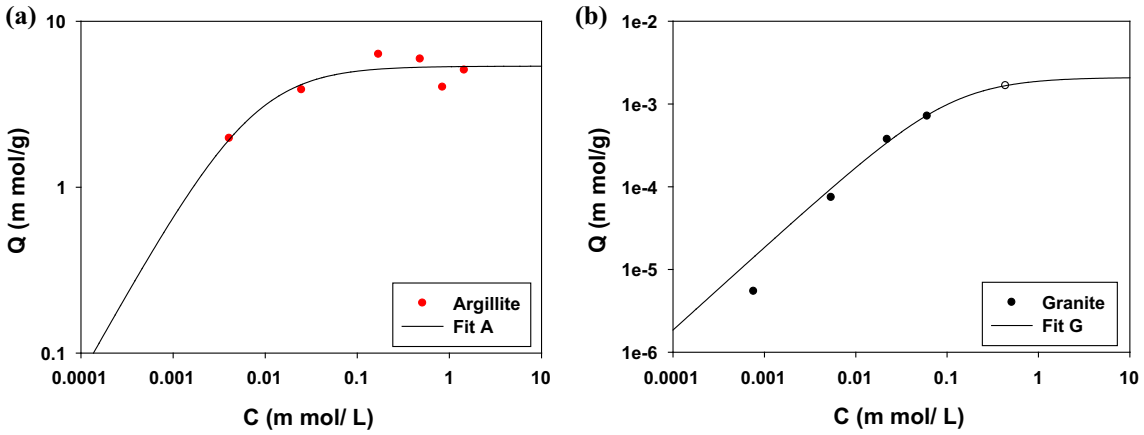

Fig. 4 Langmuir-plots of Cs sorption for **a** argillite and **b** granite

Table 3 The parameters of Langmuir isotherm models obtained from agrillite and granite

Parameter	Argillite	Granite
K (cm^3/mol)	138.797	8.8488
M (m mol/g)	5.3708	0.0021
R-square	0.9498	0.9995

compacted crushed argillite and granite with a fixed length ($L = 2$ cm). If a compacted layer is assumed to be homogeneous, isotropic and the diffusion of Cs occurs only in the x-direction, the diffusion equation can be written as Eq. (2):

$$\frac{\partial C}{\partial t} = D_a \frac{\partial^2 C}{\partial x^2}, \tag{2}$$

where C_0 and C are the initial and concentration of Cs at time t, respectively; D_a is apparent diffusion coefficients.

As $t \to \infty$, the diffusion process reach equilibrium (steady-state), and the corresponding concentration ratio (C/C_0) displays a straight line with a slope (m) and an intersection (t_x), respectively. Therefore, a graphical method [10] developed in 1975 by Crank is often employed to determine the apparent diffusion coefficient (D_a), effective diffusion coefficient (D_e), retardation factor (R_f), and distribution coefficients (K_d) from the values of m, V, L, A, t_x, ρ_b, and θ [4–6]

$$D_a = \frac{L^2}{6t_x}, \tag{3}$$

$$D_e = \frac{m \cdot V \cdot L}{A}, \tag{4}$$

$$R_f = D_e/\theta D_a. \tag{5}$$

After pre-treatment, the crushed rock samples were compacted into independent columns (duplicate tests, total 4 columns) with a bulk density (ρ_b) of 1.45 cm^3/g and a total porosity (θ) of 0.45. As started through-diffusion experiments, total volume (V) of samples on both ends (source and diffusion ends) were removed and collected at a constant frequency for detecting Cs concentration. After removing samples from two diffusion chambers, the same volume were refilled into two chambers to maintain initial condition at the boundary of $C(0,t) = C_0$.

Table 4 Diffusion parameters of HTO and Cs in compacted rocks with crushed and intact granite and argillite from through-diffusion column tests

Item	HTO				Cs			
	A2	A3	G1	G2	A2	A3	G1	G2
V	94	88	75	95	94	88	75	95
$D_a \times 10^{-10}$ (m^2/s)[a]	8.02	9.24	7.65	11.0	0.28	0.37	5.42	8.97
$D_e \times 10^{-10}$ (m^2/s)[b]	3.46	5.59	4.39	4.30	3.65	4.89	5.01	7.13
R_f	0.96	1.35	1.27	0.87	29.14	29.19	2.06	1.77
t_d	1.64	1.40	1.16	1.66	0.48	0.55	0.58	0.97

$\rho_b = 1.45$ g/cm^3; $\theta = 0.45$; $L = 2$ cm; $S = 19.6$ cm^2

$R_f = D_e/\theta D_a$

[a] $D_a = L^2/6t_x$

[b] $D_e = mVL/S$

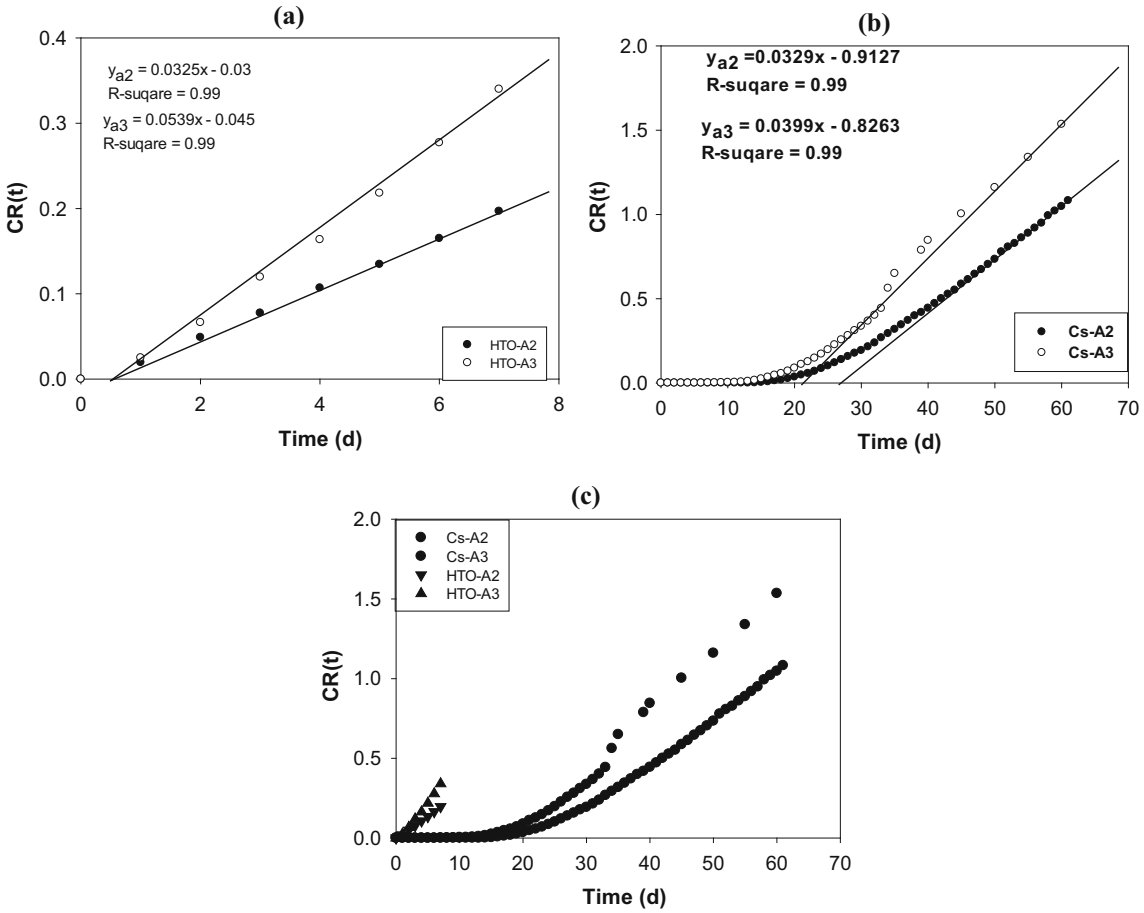

Fig. 5 Through-diffusion experiments of HTO and Cs for argillite **a** HTO, **b** Cs, **c** HTO and Cs

Results and discussion

Polar morphology and Cs sorption in SEM EDS analysis

According to the photos in polar microscopy, there are smaller crystalline particles in argillite than granite in Fig. 2 because argillite is low metamorphic rock from sedimentary rocks. Moreover, the color of clay minerals content in argillite showed black both in planed and crossed polarized light and it is easily to find out that quartz and feldspar is slightly white and grey-white, and mica is brown or orange in crossed polarized light. Furthermore, the corresponding images of SEM–EDS and Cs mapping analysis in Fig. 3 were obtained and compared, respectively. Comparison of the green area shown in Fig. 3c, f of the mineral components in argillite and granite responsible for the sorption of Cs shows that biotite and illite is a major mineral component and it also has been reported in previous studies by different analysis instruments [11–13].

Sorption of Cs on argillite and granite

According to previous studies [14, 15], Cs sorption belongs to fast-uptake reaction and reaches equilibrium within 24 h. After 7 days, the pH of Cs on argillite and granite reached equilibrium and were recorded as approximately 8.43 ± 0.2 and 7.74 ± 1.1, respectively, and showed a *Eh* within the 150–220 mV range in various particle sizes. Table 2 displays that similar batch test results indicate that K_d in argillite is higher than that in granite at the three sizes (0.149–0.833, 0.074–0.149, and <0.074 mm). In fact, the specific surface area (SSA) of crushed argillite and granite by N_2-BET increased from 6.44 to 9.13 m^2/g and 0.61 to 1.96 m^2/g as the particle size decreased, and higher K_d of Cs in argillite than that in granite also showed a similar relationship with SSA.

Sorption isotherm of Cs

The sorption isotherm of the Cs on argillite and granite was obtained using a wide range of initial Cs concentrations ranging from 10^{-3} to 10^{-5}M. The equilibrium concentration

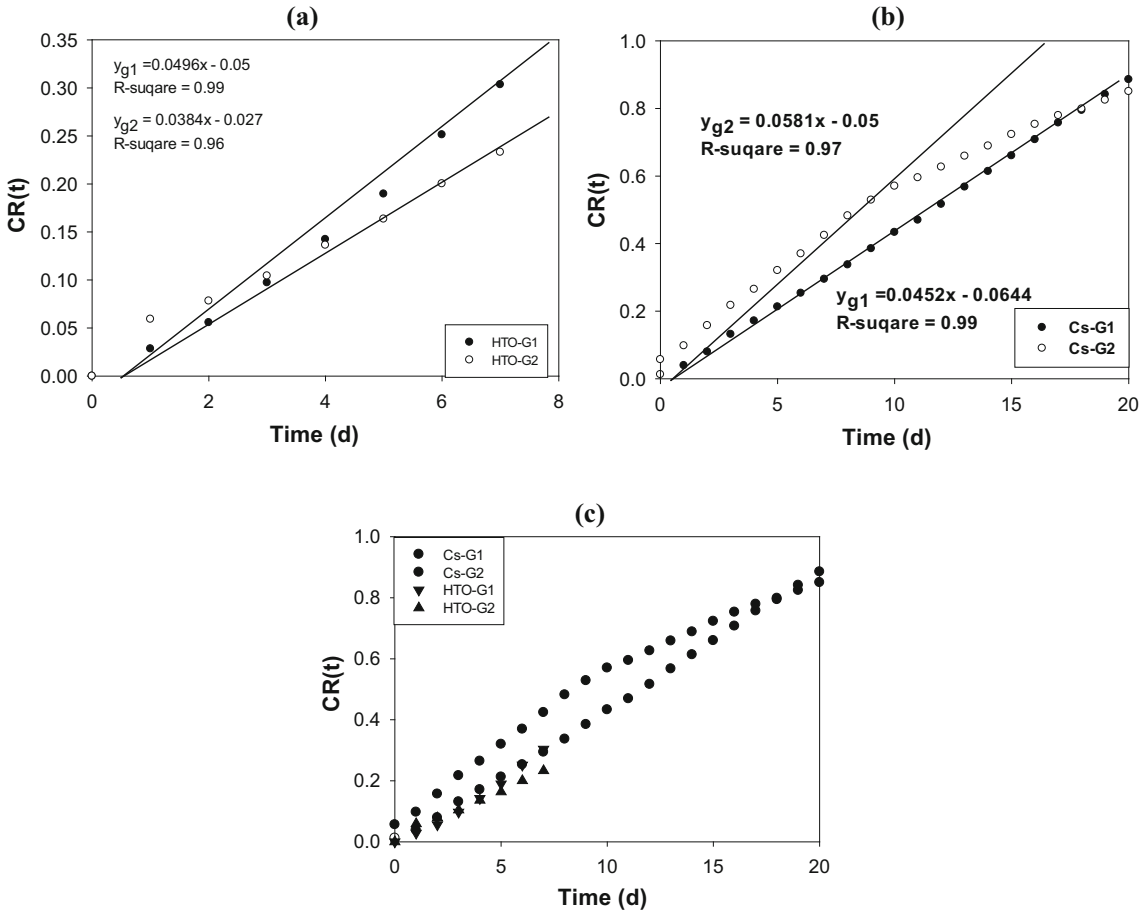

Fig. 6 Through-diffusion experiments of HTO and Cs for granite **a** HTO, **b** Cs, and **c** HTO and Cs

of the Cs adsorbed on the rocks approached a constant value with increasing Cs concentrations, suggesting that the sorption of the Cs followed a Langmuir-type sorption equation [16]. The Langmuir isotherm model is expressed as:

$$Q = \frac{MKC}{1 + KC}, \tag{6}$$

where Q and C is the equilibrium concentrations of Cs in the solid and aqueous phases. Two parameters, maximum sorption (M, m mol/g) and bonding energy coefficient (K, cm^3/mol), were used to describe the sorption capacity and the affinity of the rocks, respectively. A similar relation between Q and C was obtained from the Langmuir-plots for both rocks as seen in Fig. 4. The results shown in Table 3 indicate that the Q value of the Cs were argillite (5.3708 m mol/g) higher than granite (0.0021 m mol/g).

Steady state of Cs diffusion in argillite and granite

The apparent diffusion coefficient (D_a) and effective diffusion coefficient (D_e) could only be achieved when the through-diffusion experiments reached steady state. In other words, an important factor, the dimensionless parameter ($t_d = \frac{D_a \cdot t_f}{L^2}$), is introduced here to check whether the diffusion process reaches equilibrium. Crank (1975) [17] stated that the steady state of diffusion is achieved when t_d is higher than 0.45. In this study, the D_a, D_e, and t_d values of the experimental data shown in Table 4 for argillite and granite are all higher than 0.45, which indicates that the experimental time is sufficiently long to reach steady-state diffusion. A non-reactive tracer (HTO) was applied to understand the effect by column geometry [3, 4] and retardation factor (R_f) in argillite and granite were approximately 1 showed there is a few experimental variation from column effect in this study.

Diffusion coefficients for argillite and granite

The diffusion parameters calculated from Eqs. (3), (4) and (5) are listed in Table 4, summarizing the through-diffusion experiments on compact argillite and granite.

In addition, the accumulative concentration curves (CR(t)) for argillite and granite obtained by through-diffusion tests for HTO and Cs are shown in Figs. 5 and 6. This indicates that the time lag between HTO and Cs in

argillite to diffuse out is approximately 20 days. The through-diffusion tests showed a high *R*-square value (>0.9) in each column and exhibited obvious retardation behavior in argillite. Moreover, Table 4 shows the lowest diffusion coefficients (A2 and A3 $D_a = 2.8 \times 10^{-11}$ m^2/s and 3.7×10^{-11} m^2/s)in argillite than those in other columns. These results indicate that argillite has a higher retardation effect than granite. In fact, in addition to the microporous structure (porosity), it also identified that the major retardation of Cs in argillite depended on major sorption minerals (illite) in agreement with SEM–EDS and batch experiments.

Conclusions

The sorption properties of Cs as well as its characterization and sorption properties were investigated by using batch and SEM–EDS experiments. The sorption of Cs for argillite was higher than granite due to clay minerals content (illite) and the similar results also was demonstrated in through-diffusion tests.

Acknowledgments This work was mainly supported by the Ministry of Education, Taiwan, R.O.C. under the NCKU Aim for the Top University Project Promoting Academic Excellence and Developing World Class Research Centers. The experimental section of this study was supported by the Ministry of Science and Technology (MOST, Taiwan) under contract numbers 103-2221-E-006-227 and 105-2914-I-006-004-A1 and the Atomic Energy Council (AEC, Taiwan) through a 2015 mutual fund program project under contract number 104-NU-E-006-002-NU.

References

1. Taiwan Power Company (2009) Preliminary technical feasibility study for final disposal of spent nuclear fuel—2009 progress report (summary). Taiwan
2. Lee CP, Lan PL, Jan YL, Wei YY, Teng SP, Hsu CN (2006) Sorption of cesium on granite under aerobic and anaerobic conditions. Radiochim Acta 94:679–682
3. Lee CP, Lan PL, Jan YL, Wei YY, Teng SP, Hsu CN (2008) Sorption and diffusion of HTO and cesium in crushed granite compacted to different lengths. J Radioanal Nucl Chem 275:371–378
4. Tsai TL, Lee CP, Lin TY, Wei HJ, Men LC (2010) Evaluation of sorption and diffusion behavior of selenium in crushed granite by through-diffusion column tests. J Radioanal Nucl Chem 285:733–739
5. Lee CP, Wu MC, Tsai TL, Wei HJ, Men LC, Lin TY (2012) Comparative study on retardation behavior of Cs in crushed and intact rocks: two potential repository host rocks in the Taiwan area. J Radioanal Nucl Chem 293:579–586
6. Lee CP, Wei YY, Tsai SC, Teng SP, Hsu CN (2009) Diffusion of cesium and selenium in mudrock. J Radioanal Nucl Chem 275:761–768
7. Lee CP, Liu CY, Wu MC, Pan CH, Tsai TL, Wei HJ, Men LC (2013) Simulation of a 2-site Langmuir model for characterizing the sorption capacity of Cs and Se in crushed mudrock under various ionic strength effects. J Radioanal Nucl Chem 296:1119–1125
8. Horie K, Hidaka H, Gauthier-Lafaye F (2008) Elemental distribution in apatite, titanite and zircon during hydrothermal alteration: durability of immobilization mineral phases for actinides. Phys Chem Earth 33:962–968
9. ASTM (2010) Standard test method for distribution coefficients of inorganic species by the batch method. The American Society for Testing and Materials, C1733-10
10. Tsai SC, Ouyang S, Hsu CN (2001) Sorption and diffusion behavior of Cs and Sr on Jih-Hsing bentonite. Appl Radiat Isot 54:209–215
11. Sawhney BL (1972) Selective sorption and fixation cations by clay minerals: a review. Clays Clay Miner 20:93–100
12. Mckinley JP, Zachara JM, Heald SM, Dohnalkova A, Newville MG, Sutton SR (2004) Microscale distribution of cesium sorbed to biotite and muscovite. Environ Sci Technol 38:1017–1023
13. Benedicto A, Missana T, Fernandez AM (2014) Interlayer collapse effects on cesium adsorption onto illite. Environ Sci Technol 48:4909–4915
14. Payen TE, Bertram WK, Itakura T (2002) Relationship of quantitative X-ray diffraction measurements of geologic materials to Cs sorption. Radiochim Acta 90:705–711
15. Bostick BC, Vairavamurthy MA, Karthikeyan KG (2002) Cesium sorption on clay minerals: an EXAFS spectroscopic investigation. Environ Sci Technol 36:2670–2676
16. Benes P, Majer V (1980) Trace chemistry of aqueous solutions. Elsevier Scientific Publishing Company, Amsterdam
17. Crank J (1975) The mathematics of diffusion. Claredon Press, Oxford